*J. Anat.* (2007) **210**, pp684–692 doi: 10.1111/j.1469-7580.2007.00731.x

REVIEW

# GFP imaging of live astrocytes: regional differences in the effects of ischaemia upon astrocytes

Clare Shannon, Mike Salter and Robert Fern

*Department of Cell Physiology and Pharmacology, University of Leicester, Leicester, UK*

## Abstract

The basic division between white matter 'fibrous' astrocytes and grey matter 'protoplasmic' astrocytes is well established in terms of their morphological differences. The availability of transgenic animals with green fluorescent protein (GFP) expression restricted to specific glial cell types now provides an approach for looking at changes in cell number and morphology in the two astrocyte types in whole mount preparations. This is an important goal, as the ease of generating astrocyte cultures has led to a proliferation of studies that have examined ischaemic effects on astrocytes *in vitro*. This has in turn engendered a belief that astrocytes have an extraordinary resistance to ischaemic injury, a belief that runs counter to almost all the data available from *in vivo* and whole-mount preparations. One possible source of this confusion is the reactive changes that occur in astrocytes following injury, which include an increase in cell number that may obscure early astrocyte cell death and which has been reported to initiate within hours of an ischaemic event. However, we show here that neither white matter nor grey matter GFP(+) astrocytes exhibit any feature of reactive astrocytosis within a 180-min period of reperfusion following modelled ischaemia in neonatal whole-mount preparations. We also show that white matter astrocytes are much more sensitive to ischaemia-reperfusion injury than are grey matter astrocytes, a feature that may have high significance for developmental disorders of white matter tracts such as cerebral palsy.

**Key words** gliosis; grey matter; ischaemia; reactive; white matter.

## Introduction: astrocytes are more sensitive to ischaemic injury than you think

An interruption in the blood supply to the brain lasting for more than a few minutes will result in cell death involving both neurons and glial cells. A significant proportion of that cell death will involve astrocytes, a fact that has been obfuscated by the wide application of cell culture techniques to the examination of the relative sensitivity of brain cell types to ischaemia. Such *in vitro* studies have repeatedly shown that cultured astrocytes are much more resistant to modelled ischaemia than are cultured neurons (e.g. Goldberg & Choi, 1993). However, it is well established that even short periods of global brain ischaemia that are just sufficient to kill the brain's most ischaemia-sensitive neurons also produce a degree of astrocyte death (Petito, 1986; Petito et al. 1998), while several studies using short periods of modelled ischaemia produced regions of astrocyte injury with little collateral neuronal damage (Garcia et al. 1993; Schmidt-Kastner et al. 1993). Consistent with this, a careful examination of the literature shows that most astrocytes *in vivo* are only marginally less sensitive to acute ischaemic injury than are neurons when injury is assessed using reliable ultrastructural or immunostaining techniques (see Table 1, and Fern, 2001 for a review). For example, lesions that follow relatively brief focal ischaemia involve a significant degree of astrocyte death (Garcia et al. 1993; Schmidt-Kastner et al. 1993; Davies et al. 1998), while brief periods of global ischaemia produce a reduction in the astrocyte marker glial fibrillary acidic protein (GFAP) assessed 2 days post-injury (Petito & Halaby, 1993), correlating with the presence of dead

Correspondence
*Dr Bob Fern, Department of Cell Physiology & Pharmacology, University of Leicester, PO Box 138, University Road, Leicester LE1 9HN, UK. T: +44 (0)116 2523098; F: +44 (0)116 2525045; E: RF34@le.ac.uk*

Accepted for publication *29 March 2007*

**Table 1** Astrocyte injury evoked by ischaemic-type conditions *in vitro*, in whole mount, and *in vivo*

| Species, age | Preparation | Ischemia model | Astrocyte Injury | Method | References |
|---|---|---|---|---|---|
| | | ***In vitro*** | | | |
| Mouse, neonatal | Cultured from cortex, 14–28 DIV | OGD, 6 h + 1 day reperfusion | ~50% death | LDH release | (Goldberg & Choi, 1993) |
| Rat, foetal | Cultured from cortex, 19–21 DIV | OGD, 8 h + 1 day reperfusion | 50% death | LDH release | (Zhao & Flavin, 2000) |
| Rat, foetal | Cultured from hippocampal, 19–21 DIV | OGD, 2 h + 1 day reperfusion | 50% death | LDH release | (Zhao & Flavin, 2000) |
| Mouse, neonatal | Cultured from cortex, 21–30 DIV | Glucose deprivation, 12–18 h + 1 day reperfusion | 50% death | LDH release | (Papadopoulos et al. 1997) |
| Mouse, neonatal | Cultured from cortex, 7–27 DIV | OGD, 8–12 h + 1 day reperfusion | 50% death | LDH release | (Papadopoulos et al. 1998) |
| Rat, neonatal | Cultured from whole brain, 12–21 DIV | Hypoxia–hypoglycaemia, 6 h + 3 days reperfusion | 50% death | LDH release | (Lyons & Kettenmann, 1998) |
| | | **Whole mount** | | | |
| Rat, P2 | Whole mount optic nerve | OGD, 80 min | ~50% death | Live imaging | (Fern, 1998) |
| Rat, P10 | Whole mount optic nerve | OGD, 45 min | ~22% death | Live imaging, EM | (Thomas et al. 2004) |
| | | ***In vivo*** | | | |
| Rat, adult | Cortex | MCAO, 30 min | Process loss | IHC | (Davies et al. 1998) |
| Rat, adult | Cortex | MCAO, 60 min | Cellular disintegration | IHC | (Davies et al. 1998) |
| Rat, adult | Hippocampus | Global ischaemia, 10 min + 1 day reperfusion | Some astrocyte death | IHC | (Petito et al. 1998) |
| Rat, adult | Hippocampus | Global ischaemia, 2–30 min + 1 day reperfusion | Loss of GFAP reactivity | EM | (Petito & Halaby, 1993) |
| Rat, adult | Pre-optic area | MCAO, 30 min | Cytoplasmic disintegration | IHC | (Garcia et al. 1993) |
| Rat, adult | Cortex, basal ganglia | MCAO, 2 h + 4 h reperfusion | Loss of GFAP reactivity | IHC | (Chen et al. 1993) |
| Neonatal pig | Putamen | Hypoxia–ischaemia, ~40 min + 24–48 h reperfusion | ~50% loss of GFAP(+) cells | IHC | (Martin et al. 1997) |
| Hypertensive rat, adult | Cortex | MCAO, 1–12 h | Loss of S-100, GFAP protein and mRNA | IHC | (Liu et al. 1999) |
| Rat, adult | Cortex | MCAO, 1–3 h | Loss of GFAP mRNA | ISH | (Yamashita et al. 1996) |
| Rat, adult | Visual cortex | Photocoagulation, 4 h | Cytoplasmic disintegration | IHC | (Schmidt-Kastner et al. 1993) |

OGD = oxygen glucose deprivation, IHC = immunohistochemistry, GFAP = glial fibliary acidic protein, MCOA = middle cerebral artery occlusion, EM = electron microscopy, DIV = days *in vitro*.

astrocytes at the injury site (Petito et al. 1998). It is consistent with this that approximately half of white matter astrocytes maintained within the isolated neonatal optic nerve die after a 45–80-min period of oxygen–glucose deprivation (OGD) (Fern, 1998; Thomas et al. 2004), which is not dissimilar to the time required to kill cultured neurons (see Fern, 2001 for a review).

## Reactive astrocytosis may obscure acute astrocyte injury

There is evidence that a population of astrocytes may remain viable within the core of an ischaemic event (Thoren et al. 2005), and in transgenic animals where the fluorescent protein green fluorescent protein (GFP) is under the control of the astrocyte-specific promoter GFAP we often observed a small population of astrocytes that survive 40–60 min of OGD (see Figs 1 and 2). Such cells, together with cells in the penumbra region surrounding the lesion core, may provide the substrate for the reactive astrocytosis that is a cardinal feature of the post-ischaemic brain. This phenomenon is characterized by an increase in astrocyte number, somata volume and GFAP content (Ridet et al. 1997). There are reliable ultrastructural reports that early reactive changes are apparent in astrocytes within 15 min of the onset of an ischaemic event and that features of astrocyte cell division are seen within 180 min (Petito, 1986), although numerous immunostaining studies consistently report a much slower onset of reactive changes (e.g. Davies et al. 1998). The early timing of

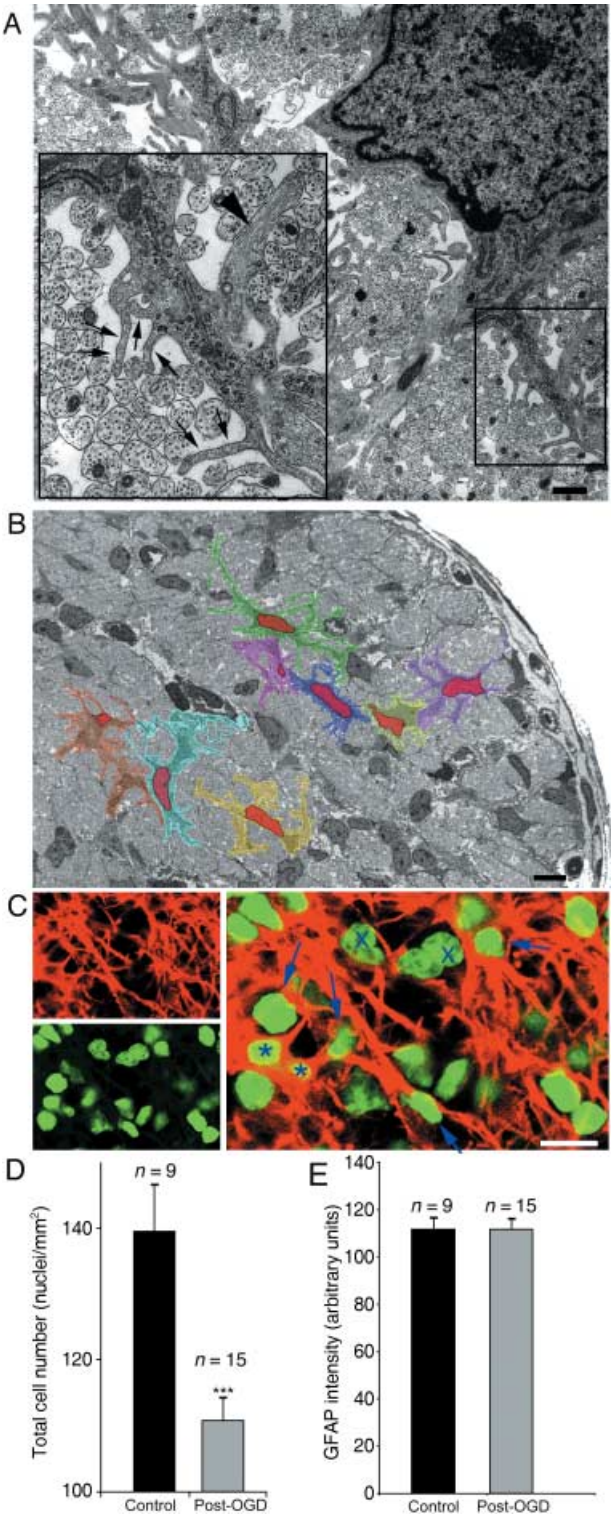


**Fig. 1** The problems of studying morphological changes in white matter astrocytes. (A) Electron micrograph of a P10 optic nerve astrocyte showing the morphological complexity of the cell. Finger processes (arrows) are as small as 50 nm and while thicker secondary processes may contain glial filaments (arrowhead), the finger processes do not. Note the other cytoplasmic features of developing white matter astrocytes that include thick endoplasmic reticulum, glycogen rosettes and a dark cytoplasm (see Thomas et al. 2004 for details). (B) Low-power micrograph of the P10 optic nerve in cross-section. Note the numerous glial cell somata. Eight astrocytes identified at higher gain have been coloured and their nuclei shaded red. Note the similarity of the thick processes to the somata in places, the close apposition of astrocyte membranes and the thinness of the cytoplasmic layer around the nucleus in places. (C) Top, left: GFAP straining of a long section of the P10 optic nerve. Bottom, left: Nuclei staining of the same section using Sytox Green. Right: overlay, showing the scarcity of positively identified astrocytes using this kind of approach (asterisk) and the numerous cells that cannot be positively localized with GFAP (e.g. arrows). Putative oligodendroglia are indicated by crosses. (D) Cell counts (nuclei) of control and post-30 min OGD optic nerve showing a significant decline in cell number following the challenge. (E) GFAP intensity measured in the whole optic nerve sections, which shows no significant difference between control and post-30 min OGD.

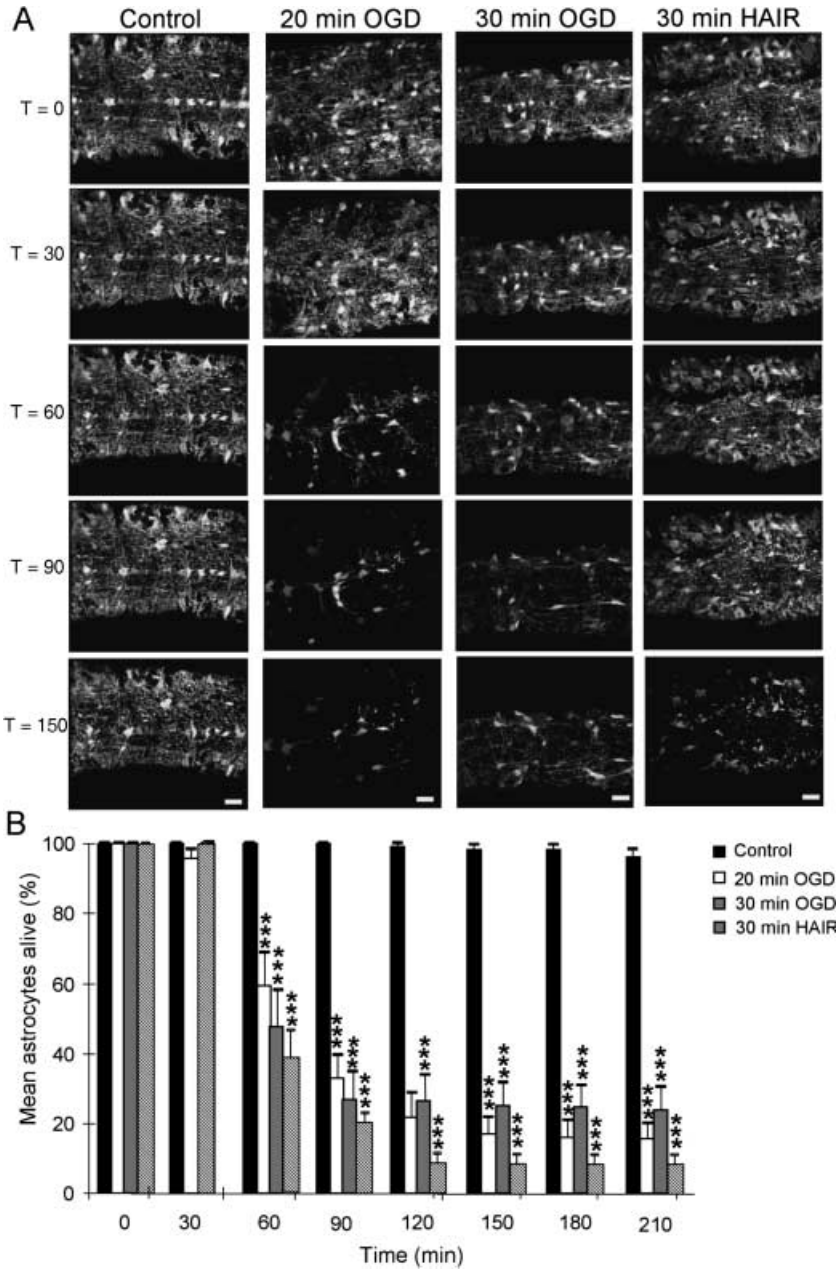


**Fig. 2** Live GFP imaging of optic nerve astrocytes. (A) Four time series of images collected from P10 optic nerves. The time series are arranged sequentially, as indicated by the times on the left (in minutes). In the control images a number of astrocyte somata can be seen at T = 0 in addition to surrounding glial processes. The cells are largely unchanged over the time course of recording. In the 20-min OGD series the cells apparent at T = 0 gradually disappear from the nerve with time and a similar decline in cell number is apparent following 30 min of OGD or 30 min of HAIR. (B) Quantification of cell loss in optic nerves exposed to the various conditions, each a minimum of four nerves. A significant loss of astrocytes is apparent after 60 min in all three ischaemic conditions with no subsequent rise. ***$P < 0.001$ vs. control.

reactive astrocytosis is of particular importance in developing white matter, which is subject to a spectrum of injuries that appear to be largely ischaemic in origin and which underlie cerebral palsy, a common birth disorder (Volpe, 1995; Back & Rivkees, 2004). Although there is controversy regarding the contribution of reactive astrocytosis to functional loss, it is clear that early and rapid astrocyte death during the evolution of the developing white matter lesion would be an important contributory factor to the pathophysiology of neighboring neurons and axons and that the subsequent depletion of normal astrocytes will severely jeopardize white matter function. It is also apparent that rapid astrocytosis might mask any early loss of astrocytes and disguise the importance of acute astrocyte injury when post-mortem samples are analysed.

## The problem of studying acute reactive changes in developing white matter

The question of how the morphology of white matter astrocytes respond to ischaemia can be addressed using

traditional methods such as electron microscopy (EM) or immunohistochemistry (IHC), although neither can be applied to a time series of the same cell. In terms of the level of morphological detail that can be resolved, EM is the superior technique. EM of control neonatal white matter astrocytes reveals their highly complex and ramified morphology (Fig. 1A), which includes thick primary processes, thinner secondary processes and finger processes that have a diameter of less than 50 nm in many cases. A low-power EM of the postpartum day 10 (P10) optic nerve is shown in Fig. 1(B), with eight individual astrocytes shaded in different colours to illustrate the difficulty of identifying individual astrocytes using standard microscopy techniques. It is apparent that depending upon the plane of section astrocytes may appear as nuclei with a very thin layer of cytoplasm, or that thick primary processes may be sectioned that have all the morphological features of entire astrocytes (other than lacking a nucleus). Furthermore, the frequently very close apposition of astrocytes will make it very hard to distinguish single cells at the level of light microscopy. All of these problems are apparent when GFAP is immunolabelled in long sections of the optic nerve (Fig. 1C, top left) together with the nuclei within the section (Fig. 1C, bottom right), and the images overlaid (Fig. 2C, right). At this stage in development (P10) ~50% of the cells in the optic nerve are astrocytes (Thomas et al. 2004), yet the double staining approach can positively identify only ~5% of cells as such (Fig. 1C, asterisk). Of the remaining nuclei, some will be oligodendroglia and some astrocytes, but the absence of clear GFAP staining around nuclei makes it impossible to distinguish them apart.

When this IHC approach is used to address changes in cell number, a 30-min period of OGD followed by 180 min of recovery leads to the expected fall in nuclei number within the nerve (Fig. 1D). It is not clear, however, which cells are lost from the structure and which, if any, may be dividing and increasing in number. Likewise, no difference is found in GFAP immunofluorescence in control and post-OGD nerves (Fig. 1E), which may be either due to an absence of reactive astrocytosis, or a masking of this phenomenon by a simultaneous decline in astrocyte number due to acute injury.

## The answer to the problem

The application of live cell imaging of GFP-expressing astrocytes can resolve these problems. In Fig. 2(A), GFP(+) astrocytes in isolated perfused P10 mouse optic nerve are imaged at 30-min intervals over a 210-min period. Control images (no OGD) on the left illustrate the stability of the astrocytes under these conditions, and the degree of cell viability is plotted in Fig. 2(B) showing low levels of cell death. Three ischaemic-type protocols are shown in Fig. 2, a 20- and a 30-min period of OGD followed by reperfusion for 190 and 180 min, respectively, and a 30-min period of perfusion with hypoxic acid-shifted Ringer's solution (HAIR; see Bondarenko & Chesler, 2001), which is designed to mimic the extracellular conditions known to exist in the brain during ischaemia. In all three cases the number of GFP(+) astrocytes can be seen to decline following the insult, with significant cell loss at 30–40 min post-insult in all three cases (Fig. 2B). In no case is there a subsequent rise in GFP(+) cell number in the nerves that would indicate cell division.

Previous studies that have reported early reactive astrocytosis examined the post-ischaemic hippocampus (Petito, 1986). Using perfused brain slices the GFP imaging approach can look at cell changes in these grey matter astrocytes, as shown in Fig. 3. The protoplasmic GFP(+) hippocampal astrocytes have a more restricted morphology at P10 than the fibrous optic nerve astrocytes, and are less ramified. The cells are stable during control perfusion (Fig. 3A, left), with neither 20 nor 30 min of OGD evoking any significant decline in astrocyte numbers (Fig. 3B). It would appear therefore that in the neonatal brain white matter astrocytes are far more sensitive to ischaemic injury than their grey matter equivalents. The same graph reveals no increase in astrocyte number in the 180–190 min of reperfusion after the insult, showing that the lack of acute astrocyte division is common to both brain regions.

It is apparent from Figs 2 and 3 that the GFP imaging approach not only allows cell number to be measured in a time series but also provides information about cell morphology. Figure 4(A) shows a time series of images of four P10 optic nerve astrocytes before, during and after a 30-min period of OGD. It is apparent that in addition to loss of two of these cells following the insult there is also marked loss of cell processes surrounding the somata. We have recently described a simple approach to assessing changes in the density of GFP(+) oligodendroglial processes in optic nerve (Salter & Fern, 2005), which we can also apply to astrocytes. A region of interest is drawn around a somata-free zone (Fig. 4B) and mean pixel intensity is measured and

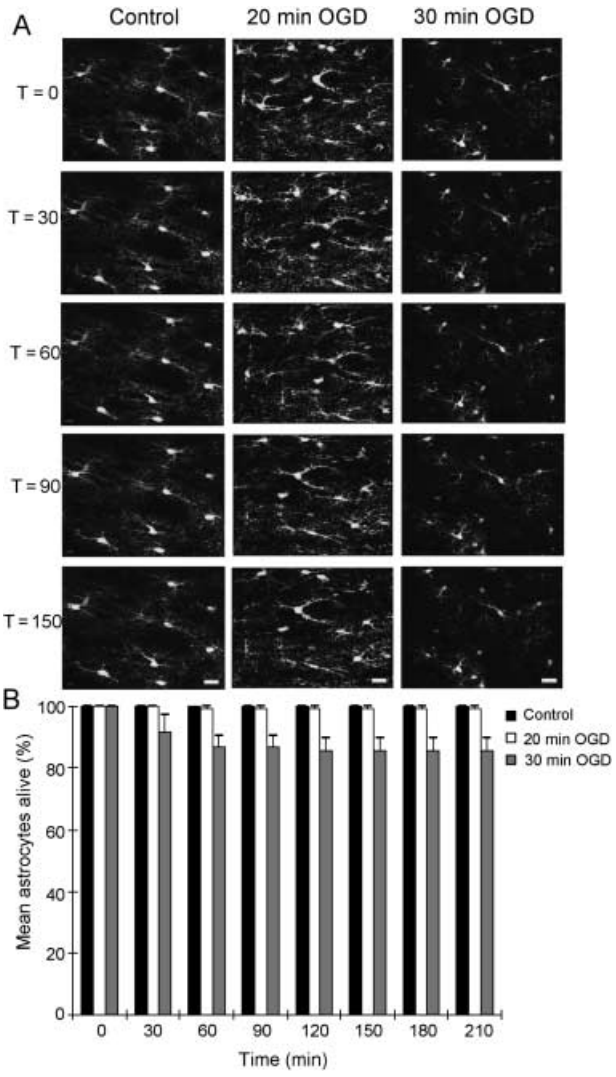


**Fig. 3** Live GFP imaging of hippocampal astrocytes. (A) Three time series of images collected from P10 hippocampal slices. The time series are arranged sequentially, as indicated by the times on the left (in minutes). In the control images a number of astrocyte somata can be seen at T = 0 in addition to surrounding glial processes. Note the greater spacing of the astrocytes compared with the optic nerve and the reduced process density. The cells are largely unchanged over the time course of recording under control, 20 min of OGD and 30 min of OGD. (B) Quantification of astrocyte loss in hippocampal slices exposed to the various conditions, each a minimum of four slices. No significant loss of astrocytes is apparent at any time point and there are no significant rises.

plotted against time (Fig. 4C). This analysis reveals marked process loss from astrocytes at 30–40 min post-OGD in both 20- and 30-min OGD experiments. There is a significantly greater degree of process loss following the longer period of OGD and in both cases the rate and degree of process loss is not significantly different from the loss of astrocyte somata shown in Fig. 2.

## Concluding remarks

The mechanisms of acute injury of neonatal white matter astrocytes depends upon the maturity of the tissue. Pre-myelinating astrocytes suffer a toxic calcium influx that is mediated mainly by voltage-gated calcium channels and leads to rapid membrane breakdown (Fern, 1998). Later in development, following the initiation of myelination, ischaemic conditions fail to produce a toxic calcium influx but instead evoke cytotoxic cell swelling that results in equally rapid loss of membrane integrity (Thomas et al. 2004). The absence of acute reactive changes at this latter developmental stage following a limited ischaemic challenge shown in the current study does not appear to be unique to the white matter given that a similar absence of reactive changes was found in their grey matter cousins. It does appear, however, that the astrocytes of actively myelinating white matter have a much heightened sensitivity to ischaemic-type injury, in particular in the reperfusion period after a brief period of an ischaemic-type condition. Differential sensitivity to ischaemic conditions between grey matter astrocyte populations are apparent in cell culture studies (Zhao & Flavin, 2000; Xu et al. 2001), although such studies always require very protracted periods of modelled ischaemia and reperfusion to generate significant cell death.

## Materials and methods for original data

Transgenic mice, strain FVB/N-Tg(GFAPGFP)14Mes/J (jax stock number 003257), carrying GFP (hGFP-S65T) under the control of the human GFAP promoter, were used for all confocal imaging studies (Zhuo et al. 1997). Heterozygous males were mated with wild-type females and transgenic litter mates identified at P4 using a blue light source and appropriate filters (the transgenic animals exhibited a characteristic green glow around their eyes). Mice aged between postnatal days 7 and 14 were decapitated and the optic nerves (MONs) were excised and placed in artificial cerebrospinal fluid (aCSF), which has a composition of (in mM): 153 $Na^+$, 3 $K^+$, 2 $Mg^{2+}$, 2 $Ca^{2+}$, 131 $Cl^-$, 26 $HCO_3^-$, 2 $H_2PO_4^-$ and 10 dextrose (see Fern, 1998). The aCSF was bubbled for at least 20 min before use with 95% $O_2$/5% $CO_2$ to

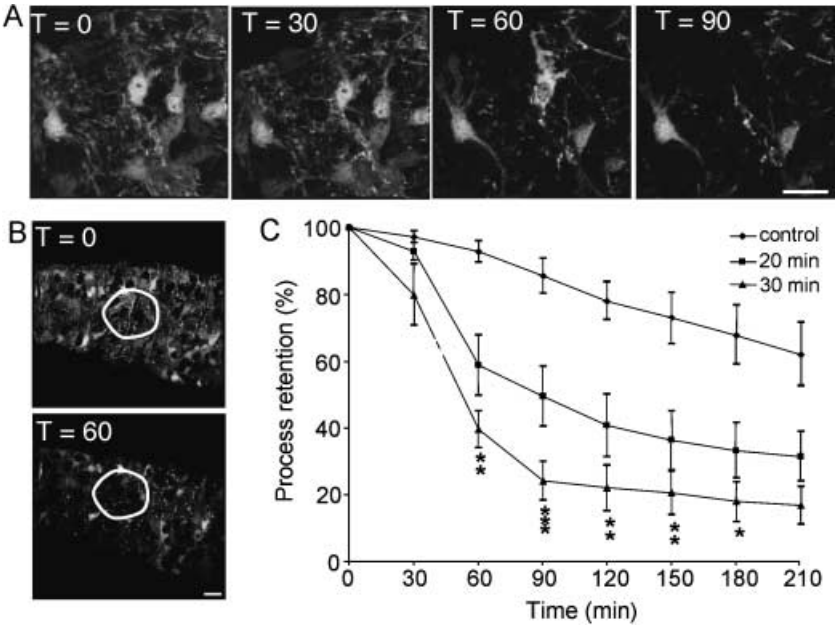


**Fig. 4** Process loss in optic nerve astrocytes. (A) A time series showing four astrocytes at T = 0 min which are surrounded by astrocyte processes. Following the termination of the 30-min period of OGD two of the astrocytes die and widespread process loss is apparent. (B) Mean pixel intensity if measured within regions of interest such as that outlined in white. (C) Loss of processes in optic nerve assessed by the decline in mean pixel intensity within regions of interest (minimum of four optic nerves). Note that process loss is rapid and severe and more extensive following the longer period of OGD. Scale bar = 10 μm.

ensure a correct pH of 7.4 and osmolarity was adjusted to 310–320 mOsmol. All procedures involving the use of animals were approved by local ethical review. Data are presented as means ± SEM and statistical significance was tested using ANOVA with Tukey's multiple comparison post-test (GraphPad Prism 4, GraphPad Software Inc.).

### Cell imaging

The ends of the optic nerves were fixed to a coverslip using a small amount of cyanoacrylate glue, leaving the majority of the nerve free of glue. The cover slip was then sealed to the bottom of a Plexiglas perfusion chamber (atmosphere chamber, Warner Instruments Corp., Hamden, CT, USA) using silicone grease (see Salter & Fern, 2005 for further details). Control conditions were maintained with continual perfusion of the above aCSF, 95% $O_2$/5% $CO_2$ as the atmosphere within the chamber and temperature regulated to 37 °C using flow-through and objective heaters (see Fern, 1998). Ischaemic conditions were simulated by switching to OGD, achieved by perfusion with glucose-free aCSF that had been bubbled with 95% $N_2$/5% $CO_2$ for a minimum of 60 min while the atmosphere within the chamber was switched simultaneously to the same gas.

The reordering chamber was mounted on the stage of an Olympus IX70 inverted confocal microscope and the MON imaged with a 60× oil-immersion objective. Once control images had been collected, the conditions were switched to OGD for either 20 or 30 min, followed by 180–190 min of reperfusion under normoxic/normoglycaemic conditions. Image stacks of 21 planes 10 μm deep were acquired every 30 min. Experiments exposing MONs to HAIR used the following solution (in mM): 34 NaCl, 13 $NaHCO_3$, 3 Na-gluconate, 65 K-gluconate, 38 NMDG-Cl, 1 Na-$H_2PO_4$, 0.13 $CaCl_2$, 1.5 $MgCl_2$, 10 glucose, pH 6.6, bubbled with 85% $N_2$/15% $CO_2$.

### Brain slices

Experiments were performed on sagittal brain slices containing the olfactory cortex, the hippocampus and surrounding axons, prepared from P10 GFAP-GFP transgenic mice. Following decapitation the brain was rapidly removed, hemisected and placed in oxygenated (95% $O_2$/5% $CO_2$) aCSF at 4 °C. A rectangular tissue block containing the olfactory cortex, hippocampus and surrounding axons was cut and stuck with cyanoacrylate glue to a metal support stage. Transverse slices (250 μm thick) were cut in bubbled ice-cold aCSF using a vibrating tissue slicer (Dosaka em company, Kyoto, Japan) and maintained in a holding chamber in oxygenated aCSF at 32 °C for 30 min before use. Only brain slices where the hippocampus could be clearly identified were used. A brain slice was then transferred to a Plexiglas perfusion chamber and held in place in the perfusion chamber using a nylon-fibre grid (harp). The protocol for cell imaging of MONs was then followed.

### Immunohistochemistry

MONs were transferred to 0.1 M phosphate-buffered saline solution (PBS) (Gibco/Invitrogen) prior to fixing in 4% paraformaldehyde for 30 min at room temperature. The nerves were then cryoprotected (20–30% sucrose for 5 min) and transferred to Tissue Tec media (Sigma) and frozen using ethanol and dry ice. Sections (20 μm) were cut by cryostat and mounted on to microscope slides. The freshly cut sections were then submerged in 0.1 M PBS for 5 min and then blocked in 0.1 M PBS containing 10% goat serum and 0.5% Triton-X for 120 min at room temperature prior to overnight exposure to monoclonal GFAP (Molecular Probes, 1 : 200) at 4 °C in the same solution. Slides were then washed (3 × 5 min) and incubated in Alexa Fluor-568-conjugated goat anti-mouse (Molecular Probes, 1 : 1000) for 60 min at room temperature. The sections were then washed sequentially in 0.5, 0.1 and 0.05 M PBS containing 10% goat serum and 0.5% Triton X prior to incubation in Sytox Green nuclear stain (Molecular Probes) at a concentration of 100 nM in 0.1 M PBS for 10 min. Images were collected using the Olympus Fluoview IX70 confocal microscope (60× objective) and analysed with Metamorph (Universal Imaging Corp., Philadelphia, PA, USA) and ImageJ (NIH). The number of nuclei in nerve sections was counted by eye in a blinded fashion.

## Acknowledgements

This work was supported by the National Institutes of Neurological Disorders and Stroke grant NS 44875 to R.F. We wish to thank Jamie Johnston and the laboratory of Ian Forsythe for help with brain slicing, and James Alix for help with the IHC.

## References

**Back SA, Rivkees SA** (2004) Emerging concepts in periventricular white matter injury. *Semin Perinatol* **28**, 405–414.

**Bondarenko A, Chesler M** (2001) Rapid astrocyte death induced by transient hypoxia, acidosis, and extracellular ion shifts. *Glia* **34**, 134–142.

**Chen H, Chopp M, Schultz L, Bodzin G, Garcia JH** (1993) Sequential neuronal and astrocytic changes after transient middle cerebral artery occlusion in the rat. *J Neurol Sci* **118**, 109–106.

**Davies CA, Loddick SA, Stroemer RP, Hunt J, Rothwell NJ** (1998) An integrated analysis of the progression of cell responses induced by permanent focal middle cerebral artery occlusion in the rat. *Exp Neurol* **154**, 199–212.

**Fern R** (1998) Intracellular calcium and cell death during ischemia in neonatal rat white matter astrocytes in situ. *J Neurosci* **18**, 7232–7243.

**Fern R** (2001) Ischemia: astrocytes show their sensitive side. *Prog Brain Res* **132**, 405–411.

**Garcia JH, Yoshida Y, Chen H, et al**. (1993) Progression from ischemic injury to infarct following middle cerebral artery occlusion in the rat. *Am J Pathol* **142**, 623–635.

**Goldberg MP, Choi DW** (1993) Combined oxygen and glucose deprivation in cortical cell culture: calcium-dependent and calcium-independent mechanisms of neuronal injury. *J Neurosci* **13**, 3510–3524.

**Liu D, Smith CL, Barone FC, et al**. (1999) Astrocytic demise precedes delayed neuronal death in focal ischemic rat brain. *Brain Res Mol Brain Res* **68**, 29–41.

**Lyons SA, Kettenmann H** (1998) Oligodendrocytes and microglia are selectively vulnerable to combined hypoxia and hypoglycemia injury in vitro. *J Cereb Blood Flow Metab* **18**, 521–530.

**Martin LJ, Brambrink AM, Lehmann C, et al**. (1997) Hypoxia-ischemia causes abnormalities in glutamate transporters and death of astroglia and neurons in newborn striatum. *Ann Neurol* **42**, 335–348.

**Papadopoulos MC, Koumenis IL, Dugan LL, Giffard RG** (1997) Vulnerability to glucose deprivation injury correlates with glutathione levels in astrocytes. *Brain Res* **748**, 151–156.

**Papadopoulos MC, Koumenis IL, Yuan TY, Giffard RG** (1998) Increasing vulnerability of astrocytes to oxidative injury with age despite constant antioxidant defenses. *Neuroscience* **82**, 915–925.

**Petito CK** (1986) Transformation of postischemic perineuronal glial cells. I. Electron microscopic studies. *J Cereb Blood Flow Metab* **6**, 616–624.

**Petito CK, Halaby IA** (1993) Relationship between ischemia and ischemic neuronal necrosis to astrocyte expression of glial fibrillary acidic protein. *Int J Dev Neurosci* **11**, 239–247.

**Petito CK, Olarte JP, Roberts B, Nowak TS Jr, Pulsinelli WA** (1998) Selective glial vulnerability following transient global ischemia in rat brain. *J Neuropathol Exp Neurol* **57**, 231–238.

**Ridet JL, Malhotra SK, Privat A, Gage FH** (1997) Reactive astrocytes: cellular and molecular cues to biological function. *Trends Neurosci* **20**, 570–577.

**Salter MG, Fern R** (2005) NMDA receptors are expressed in developing oligodendrocyte processes and mediate injury. *Nature* **438**, 1167–1171.

**Schmidt-Kastner R, Wietasch K, Weigel H, Eysel UT** (1993) Immunohistochemical staining for glial fibrillary acidic protein (GFAP) after deafferentation or ischemic infarction in rat visual system: features of reactive and damaged astrocytes. *Int J Dev Neurosci* **11**, 157–174.

**Thomas R, Salter MG, Wilke S, et al**. (2004) Acute ischemic injury of astrocytes is mediated by Na-K-Cl cotransport and not $Ca^{2+}$ influx at a key point in white matter development. *J Neuropathol Exp Neurol* **63**, 856–871.

**Thoren AE, Helps SC, Nilsson M, Sims NR** (2005) Astrocytic function assessed from 1 to 14C-acetate metabolism after temporary focal cerebral ischemia in rats. *J Cereb Blood Flow Metab* **25**, 440–450.

**Volpe JJ** (1995) *Neurology of the Newborn*. Philadelphia: W.B. Saunders.

**Xu L, Sapolsky RM, Giffard RG** (2001) Differential sensitivity of murine astrocytes and neurons from different brain regions to injury. *Exp Neurol* **169**, 416–424.

**Yamashita K, Vogel P, Fritze K, Back T, Hossmann KA, Wiessner C** (1996) Monitoring the temporal and spatial activation pattern of astrocytes in focal cerebral ischemia using in situ hybridization to GFAP mRNA: comparison with sgp-2 and hsp70 mRNA and the effect of glutamate receptor antagonists. *Brain Res* **735**, 285–297.

**Zhao G, Flavin MP** (2000) Differential sensitivity of rat hippocampal and cortical astrocytes to oxygen-glucose deprivation injury. *Neurosci Lett* **285**, 177–180.

**Zhuo L, Sun B, Zhang CL, Fine A, Chiu SY, Messing A** (1997) Live astrocytes visualized by green fluorescent protein in transgenic mice. *Dev Biol* **187**, 36–42.